

Three-dimensional effective properties of layered composites with imperfect interfaces

Hamsasew Sertse and Wenbin Yu*

School of Aeronautics and Astronautics, Purdue University, West Lafayette, Indiana 47907, U.S.A.

(Received June 2, 2017, Revised July 3, 2017, Accepted July 4, 2017)

Abstract. The objective of this paper is to obtain three-dimensional (3D) effective properties for layered composites with imperfect interfaces using mechanics of structure genome. The imperfect interface is modeled using linear traction-displacement model that allows small infinitesimal displacement jump across the interface. The predictions obtained from the current analysis are compared with the 3D finite element analysis (FEA). In this study, it is found that the present model shows excellent agreement with the results obtained using 3D FEA by employing periodic boundary conditions. The prediction also reveals that in-plane longitudinal and shear moduli, and all Poisson's ratios are observed to be not affected by the interfacial stiffness while the predictions of transverse longitudinal and shear moduli are significantly influenced by interfacial stiffness.

Keywords: mechanics of structure genome; imperfect interface; effective properties

1. Introduction

Although layered composites can be analyzed using various modeling techniques (Jayatilake *et al.* (2016), Munoz *et al.* (2015)), there are practical needs of treating it as a homogeneous solid with three-dimensional (3D) effective properties. Because of the simplicity of layered composites, it is used as a model structure to solve problems in many areas including wave propagation (Ghosh (1985), Wang (1999), Amor and Ghoslen (2007)) and structural optimization analysis (Bendsoe (1989)). It is also commonly used to obtain effective multiphysics properties of materials (piezoelectric, thermoelectric and, magneto-electric effects, magneto-electro elastic) by adopting micromechanical approaches (Braga and Herrmann (1992), Santoyoa *et al.* (2007), Chen *et al.* (2002), Kim *et al.* (2009)). The effective properties of layered composites are analyzed using various approaches including averaging method (Backus (1962)), rules of mixtures (Lim (2009)) and analytical approaches (Norris (1990), Kim (2001)). Manevitch *et al.* (2002) employed mathematical homogenization theory proposed by Bensoussan *et al.* (1978) to obtain the effective properties of layered composites. An extensive treatment on layered composites can be found in Milton Milton (2002). Yu (2012, 2016) recently used the variational asymptotic method to obtain an exact solution for layered composites. Lebee and

*Corresponding author, Professor, E-mail: wenbinyu@purdue.edu

Sab (2010) used higher order terms to analyze both the effective properties and local fields of layered composites. Cecchi and Sab (2007) obtained the effective properties of layered composites using various homogenization approaches. Lan and Wei (2012) analyzed the effect of imperfect interface on the local field distribution of laminated piezoelectric plate. This work assumes only transverse displacement jumps, which may not be reasonable for various loading options including shear loading. Massabo and Campi (2015) used a zigzag plate theory to predict the effects of imperfect interfaces on the local field distributions. Kim *et al.* (2011) developed a higher-order zigzag theory to analyze the effect of imperfect interface. In this case, only the in-plane displacement jumps, i.e., slip, was considered. Similarly, Kamali and Pourmoghaddam (2016) used only the in-plane displacement jump to analyze the effect of imperfect interface on local field distributions. In-plane slip is important, however the transverse displacement jump is also equally critical to rigorously predict the effective properties of layered composite. Alvarez-Lima *et al.* (2012a, b) modeled imperfect interfaces using a thin adhesive layer with specific material properties, where the interface exhibits elastoplastic behavior. It is possible to use a thin layer to account for imperfect interfaces, but the properties of the thin layer is not easily quantifiable. Despite extensive works, none of them considered the effect of an imperfect interface between the layers for predicting a complete set of effective properties.

In layered composites, as two or more alternating anisotropic layers are bonded together (see Fig. 1), it natural to expect that the layers may not be perfectly bonded due to various factors such as manufacturing defects, inherent properties of the layers and bonding agents. Hashin (1991a) demonstrated the effect of an imperfect interface on the effective properties of composite. For layered composites, although various approaches proposed to obtain the effective properties, all of them are performed by assuming a perfect interface between the layers, which might not be valid due to aforementioned factors. Thus, the effect of an imperfect interface is of interest to better characterize the effective properties of a layered composite. Numerous efforts have been devoted to

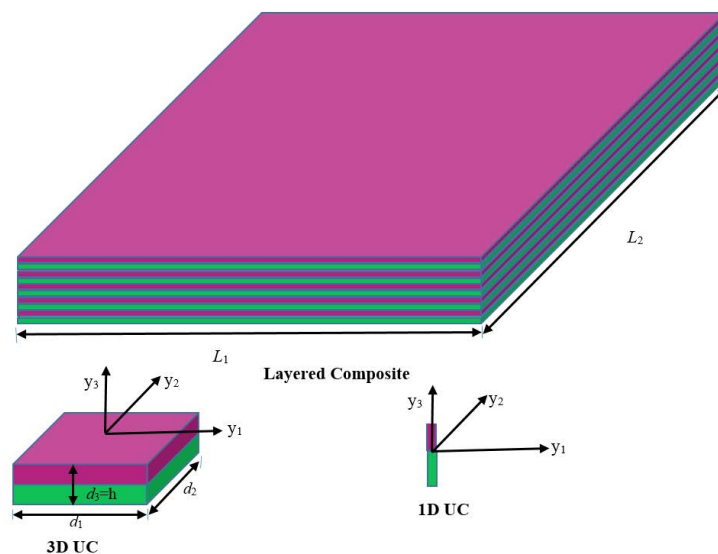


Fig. 1 Sketch of a layered composite

develop constitutive models that adequately capture the effect of imperfect interfaces on the effective properties and the failure strength of the composites. Jones and Whittier (1967) proposed a linear interface model, where the interfacial traction is proportional to the displacement jumps across the interface. On the other hand, Le-Quang and He (2008) employed the stress jump assumption to obtain effective properties. This assumes stress jumps across interface while the displacement remains to be continuous. In this case, the static interfacial equilibrium is maintained by the generalized Young-Laplace equation. Various interfacial constitutive models have been proposed and widely used to analyze the effect of imperfect interfaces on the properties of composite materials (Bednarczyk and Arnold (2001)).

The objective of the current study is to obtain exact solutions of effective properties for layered composites with imperfect interfaces using mechanics of structure genome (MSG). The imperfect interface is modeled using the linear traction-displacement model that allows small infinitesimal displacement jump across the interface. The predictions obtained from the current analysis are compared with the predictions obtained representative volume element (RVE) analysis, 3D FEA.

2. Interfacial constitutive model

For the present study, let the interfaces among different layers be subjected to infinitesimal displacement jumps across the interface. The linear traction-displacement model can then be adopted to analyze the effect of imperfect interface (Hashin (1991a)). The linear traction-displacement model may be expressed as

$$T_i = D_{ij}[u_j], \quad [u_j] = u_j^1 - u_j^2 \quad (1)$$

where T_i denote the interfacial tractions, the square brackets denote the difference of the function evaluated below and above the interface, the commonly called jump conditions, D_{ij} denote the second-order interface constitutive tensor (interface stiffness with unit Pa/m). The interfacial displacement jumps can be expressed using three modes. Let the infinitesimal displacement jump normal to the interface in y_3 direction be captured by interfacial stiffness D_I , and let the two displacement jumps in the plane of the interface ($y_1 - y_2$ plane) be expressed for y_1 and y_2 directions using interfacial stiffness D_{II} and D_{III} , respectively. One of the basic and necessary assumption in the homogenization of heterogeneous materials is that the exact solutions of the field variables have volume averages over the unit cell. For example, if u_i are the exact displacements within the unit cell, there exist v_i such that

$$v_i = \frac{1}{\Omega} \int_{\Omega} u_i d\Omega = \langle u_i \rangle \quad (2)$$

where Ω denotes the domain occupied by a unit cell volume, and $\langle \bullet \rangle$ denotes the volume average over Ω . Here and throughout the paper, Latin indices assume 1, 2, and 3 and repeated indices are summed over their range except where explicitly indicated. Using Eq. (2), we can express the exact solution as a sum of the volume average and the difference, such that

$$u_i(x, y) = v_i(x) + \chi_i(x, y) \quad (3)$$

where $\chi_i(x, y)$ is usually called the fluctuating function. Using Eqs. (2) and (3), one can obtain $\langle \chi_i \rangle = 0$. Similarly, using Eq. (3), the displacement jump $[u_j]$ can be rewritten as

$$[u_i] = [\chi_i] \quad (4)$$

Using Eqs. (1) and (4), the strain energy due to interfacial displacement jump can be expressed as

$$U_{int} = \frac{1}{2\gamma} \int_{\gamma} [\chi]^T D[\chi] d\gamma = \frac{1}{2} \langle [\chi]^T D[\chi] \rangle^* \quad (5)$$

where γ is the interfacial area, and $\langle \bullet \rangle^*$ denote averaging over the interface area. In this analysis, D is assumed to be diagonal tensor or mode independent, i.e., displacement jump in one direction does not affect the displacement jump in the other two directions. It is also assumed that the interfacial deformation remains to be elastic, i.e., no interfacial damage.

3. Mechanics of structure genome (MSG) - based micromechanics

MSG provides a general-purpose micromechanics theory when it is applied to constitutive modeling of 3D structures. The term genome is used to emphasize the fact that it contains all the constitutive information needed for a structure the same fashion as the genome contains all the intrinsic information for an organism's growth and development. For 3D bodies, A SG serves a similar role as a RVE or unit cell (UC) concept in micromechanics (see Fig. 2). However, they are different. For example, for a structure made of composites featuring 1D heterogeneity (e.g., binary composites made of two alternating layers, see Fig. 1 and Fig. 2(a)), the SG will be a straight line with two segments denoting corresponding different layers. Interested reader can refer to Yu (2016) for more details on MSG. A 3D SG for 3D structures represents the most similar case to RVE. However, boundary conditions in terms of displacements and tractions indispensable in RVE-based models are not needed for SG-based models. MSG is developed based on the principle of minimum information loss which states that the homogenized model can be constructed through minimizing the information loss between the original heterogeneous body and the homogenized body. For a linear elastic material, the information can be the strain energy density. According to MSG, we need to first express the kinematics of the original heterogeneous body in terms of that of the homogeneous body as

$$u_i(x, y) = v_i(x) + \chi_i(x, y) \quad (6)$$

where u_i denotes the displacement field of the heterogeneous materials, v_i denotes displacement field of homogenized body, and χ_i denotes the difference between these two fields, x and y denote macro and micro coordinates, respectively. Then one can obtain the strain field of the heterogeneous body as

$$\varepsilon_{ij}(x, y) = \bar{\varepsilon}_{ij}(x, y) + \frac{1}{\delta} \chi_{(i,j)} \quad (7)$$

Here $\chi_{(i,j)}$ denotes the symmetric gradient of χ_i with respect to the micro coordinates. The higher order terms have been neglected according to the variational asymptotic method (Berdichevsky (2009), Wang and Yu (2014)). For constructing the homogenized model out of the original model,

one needs to define the kinematic variables of the homogenized model in terms of those of the original model. The natural choice is to define

$$\bar{u}_i = \langle u_i \rangle = v_i, \quad \bar{\varepsilon}_{ij} = \langle \varepsilon_{ij} \rangle \tag{8}$$

which implies the following constraints on the fluctuating functions

$$\langle \chi_i \rangle = 0, \quad \langle \chi_{(i,j)} \rangle = 0 \tag{9}$$

The angle brackets denote averaging over the SG. The principle of minimum information loss seeks to minimize the difference between the strain energy of the original model and the homogenized model. External load is unnecessary to obtain effective properties in this approach, unlike 3D FEA. In the current study, the original model includes the interfacial energy, thus the principle of minimum information loss can be expressed as

$$\Pi = \left\langle \frac{1}{2} C_{ijkl} (\bar{\varepsilon}_{ij} + \chi_{(i,j)}) (\bar{\varepsilon}_{kl} + \chi_{(k,l)}) \right\rangle + \frac{1}{2} \langle [\chi_i]^T D_{ij} [\chi_j] \rangle^* - \frac{1}{2} C_{ijkl}^* \bar{\varepsilon}_{ij} \bar{\varepsilon}_{kl} \tag{10}$$

where C_{ijkl} denote the fourth-order elasticity tensor. To minimize the strain energy Π , one considers the homogenized model as given (i.e., C_{ijkl}^* , $\bar{\varepsilon}_{ij}$ cannot be varied). Then χ_i can be solved from the following variational statement

$$\min \Pi = \min_{\chi_i \in Eq(9)} \left\{ \left\langle \frac{1}{2} C_{ijkl} (\bar{\varepsilon}_{ij} + \chi_{(i,j)}) (\bar{\varepsilon}_{kl} + \chi_{(k,l)}) \right\rangle + \left\langle \frac{1}{2} [\chi_i]^T D_{ij} [\chi_j] \right\rangle^* \right\} \tag{11}$$

This minimization problem is formulated for an arbitrary microstructure. For layered composites (see Fig. 1 and Fig. 2(a)), the problem, Eq. (11), can be analytically solved to obtain the exact solution. In this case, the heterogeneity only occurs through the thickness along y_3 as shown in the figures and, in $y_1 - y_2$ plane, each layer is homogeneous. Thus, χ_i are functions of y_3 only, that is, the partial derivatives of the fluctuating functions $\chi_{i,j}$ vanish except for $\chi_{i,3}$. Similarly, the interface is assumed

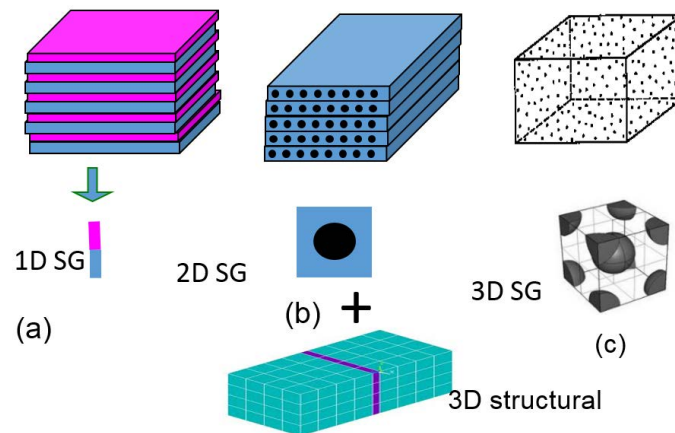


Fig. 2 SG for different dimensions

to have uniform traction and displacement jumps. The minimization problem for micromechanical analysis of layered composites with imperfect interface can be restated using a matrix form as

$$\Pi = \frac{1}{2} \langle \Gamma^T C \Gamma \rangle + \frac{1}{2} \langle [\chi]^T D [\chi] \rangle^* \quad (12)$$

with $\Gamma = \left[\begin{array}{cccccc} \bar{\varepsilon}_{11} & \bar{\varepsilon}_{22} & \bar{\varepsilon}_{33} + \frac{\partial \chi_3}{\partial y_3} & 2\bar{\varepsilon}_{23} + \frac{\partial \chi_2}{\partial y_3} & 2\bar{\varepsilon}_{13} + \frac{\partial \chi_1}{\partial y_3} & 2\bar{\varepsilon}_{12} \end{array} \right]^T$ as the microscopic strain field. The microscopic stress field within SG can be obtained as

$$\sigma = C \Gamma \quad (13)$$

with $\sigma = \left[\begin{array}{cccccc} \sigma_{11} & \sigma_{22} & \sigma_{33} & \sigma_{23} & \sigma_{13} & \sigma_{12} \end{array} \right]^T$ holding the six components of the stress tensor. By applying the normal procedures of calculus of variations and enforcing the constraints using Lagrange multipliers, one can obtain three Euler-Lagrangian equations as

$$\frac{\partial}{\partial y_3} (\sigma_{13} - D_{22}[\chi_1]) = 0, \quad \frac{\partial}{\partial y_3} (\sigma_{23} - D_{33}[\chi_2]) = 0, \quad \frac{\partial}{\partial y_3} (\sigma_{33} - D_{11}[\chi_3]) = 0. \quad (14)$$

Similarly, one can also derive the following conditions relating the transverse stresses at the boundary points of SG

$$\sigma_{i3} \left(y_1, y_2, -\frac{h}{2} \right) = \sigma_{i3} \left(y_1, y_2, \frac{h}{2} \right). \quad (15)$$

The three stress continuity conditions on each interface of the layers can be expressed as

$$[\sigma_{i3}] = 0 \quad (16)$$

Using Eqs. (14) and (16), one can obtain the relationship between the stress and displacement jumps as

$$\sigma_{13} - D_{II}[\chi_1] = 0, \quad \sigma_{23} - D_{III}[\chi_2] = 0, \quad \sigma_{33} - D_I[\chi_3] = 0. \quad (17)$$

Following the procedures described in Yu (2005, 2012) and using Eq. (9) and Eqs. (15)-(17), and assuming a periodic displacement boundary conditions in transverse direction, one can solve the problem analytically. It should be noted that only unique/representative layers are to be used for the analysis. For instance, if two layers of different material properties are repeated to generate the layered composite with n number of layers, only the 2 unique layers would be used for the analysis. First, for the simple case of two isotropic layers, the effective properties of layered composite with imperfect interface can then be obtained as

$$E_1 = E_2 = \phi_1 E^{(1)} + \phi_2 E^{(2)} + \frac{\phi_1 \phi_2 E^{(1)} E^{(2)} (\nu^{(1)} - \nu^{(2)})^2}{\phi_1 E^{(1)} (1 - \nu^{(2)^2}) + \phi_2 E^{(2)} (1 - \nu^{(1)^2})} \quad (18)$$

$$G_{12} = \frac{\phi_1 E^{(1)}}{2(\nu^{(1)} + 1)} + \frac{\phi_2 E^{(2)}}{2(\nu^{(2)} + 1)} \quad (19)$$

$$G_{13} = \frac{D_{III}^2 \phi_1 E^{(1)} E^{(2)^2} (1 + \nu^{(1)})^2 (\frac{1}{2} + \frac{1}{2} \nu^{(2)}) + D_{III} E^{(1)^2} E^{(2)} (E^{(2)} (\frac{1}{4} + \nu^{(1)} (\frac{1}{4} + \frac{1}{4} \nu^{(2)}) + \frac{1}{4} \nu^{(2)}))}{\frac{D_{III}^2 \phi_2 E^{(1)^2} E^{(2)} (\frac{1}{2} + \frac{1}{2} \nu^{(1)}) (1 + \nu^{(2)})}{M_{III}}} + \quad (20)$$

$$G_{23} = \frac{D_{II}^2 \phi_1 E^{(1)} E^{(2)2} (1+\nu^{(1)})^2 (\frac{1}{2} + \frac{1}{2} \nu^{(2)}) + D_{II} E^{(1)2} E^{(2)} (E^{(2)} (\frac{1}{4} + \nu^{(1)} (\frac{1}{4} + \frac{1}{4} \nu^{(2)}) + \frac{1}{4} \nu^{(2)}))}{\frac{M_{II}}{D_{II}^2 \phi_2 E^{(1)2} E^{(2)} (\frac{1}{2} + \frac{1}{2} \nu^{(1)}) (1+\nu^{(2)})}} + \tag{21}$$

$$\nu_{12} = \frac{\phi_1 E^{(1)} \nu^{(1)} (\nu^{(2)2} - 1) + \phi_2 E^{(2)} \nu^{(2)} (\nu^{(1)2} - 1)}{\phi_1 E^{(1)} (\nu^{(2)2} - 1) + \phi_2 E^{(2)} (\nu^{(1)2} - 1)} \tag{22}$$

$$\nu_{13} = \nu_{23} = \frac{(\nu^{(1)} \nu^{(2)} - \phi_1 \nu^{(1)} - \phi_2 \nu^{(2)}) (\phi_1 E^{(1)} (1 + \nu^{(2)}) + \phi_2 E^{(2)} (1 + \nu^{(1)}))}{\phi_1 E^{(1)} (\nu^{(2)2} - 1) + \phi_2 E^{(2)} (\nu^{(1)2} - 1)} \tag{23}$$

where $M_\alpha = (1 + \nu^{(1)})(1 + \nu^{(2)}) (-\frac{1}{2} E^{(1)} E^{(2)} (\phi_1 E^{(1)} (1 + \nu^{(2)}) - \phi_1 E^{(2)} (1 + \nu^{(1)}) - E^{(1)} (1 + \nu^{(2)})))^2$, $\alpha = III$ or II , with ϕ_i denotes the volume fraction or thickness fraction of layer i , $E^{(i)}$ and $\nu^{(i)}$ elastic modulus and Poisson's ratio of layer i . The explicit exact solutions of E_3 is very lengthy, thus they are not shown here, but it is observed to be affected by D_I . Eqs. (18)-(19), (22) and (23) are similar to the one obtained by Yu (2012) for a perfectly bonded interface. Eqs. (18)-(19), (22) and (23) show that the effective elastic modulus E_1 and E_2 , the shear modulus G_{12} , all Poisson's ratios (ν_{12} , ν_{13} , ν_{23}) are independent of interfacial stiffness, while G_{13} and G_{23} are dependent on the interfacial stiffness, D_{III} and D_{II} , respectively, as shown in Eq. (20) and Eq. (21). Second, for more general case, let the properties of layers be monoclinic. Eq. (24) shows the effective properties of monoclinic layers.

$$\mathbf{C}^* = \begin{bmatrix} C_{11}^* & C_{12}^* & C_{13}^* & 0 & 0 & C_{16}^* \\ & C_{22}^* & C_{23}^* & 0 & 0 & C_{26}^* \\ & & C_{33}^* & 0 & 0 & C_{36}^* \\ & & & C_{44}^* & C_{45}^* & 0 \\ & SYMM & & & C_{55}^* & 0 \\ & & & & & C_{66}^* \end{bmatrix}. \tag{24}$$

The components of stiffness tensor in Eq. (24) can be written as function of interfacial stiffness as shown in Eq. (25).

$$\begin{aligned} C_{11}^* &= \langle C_{11} \rangle + C_{11}^E (C^{(1)}, C^{(2)}, D_I), & C_{12}^* &= \langle C_{12} \rangle + C_{12}^E (C^{(1)}, C^{(2)}, D_I) \\ C_{16}^* &= \langle C_{16} \rangle + C_{16}^E (C^{(1)}, C^{(2)}, D_I), & C_{26}^* &= \langle C_{26} \rangle + C_{26}^E (C^{(1)}, C^{(2)}, D_I) \\ C_{22}^* &= \langle C_{22} \rangle + C_{11}^E (C^{(1)}, C^{(2)}, D_I), & C_{23}^* &= \frac{D_I (C_{23}^{(2)} C_{33}^{(1)} \phi_2 + C_{23}^{(1)} C_{33}^{(2)} \phi_1)}{(C_{33}^{(2)} \phi_1 + C_{33}^{(1)} \phi_2) D_I + C_{33}^{(2)} C_{33}^{(1)}} \\ C_{33}^* &= \frac{D_I C_{33}^{(1)} C_{33}^{(2)}}{(C_{33}^{(2)} \phi_1 + C_{33}^{(1)} \phi_2) D_I + C_{33}^{(2)} C_{33}^{(1)}}, & C_{13}^* &= \frac{D_I (C_{13}^{(2)} C_{33}^{(1)} \phi_1 + C_{13}^{(1)} C_{33}^{(2)} \phi_2)}{(C_{33}^{(2)} \phi_1 + C_{33}^{(1)} \phi_2) D_I + C_{33}^{(2)} C_{33}^{(1)}} \\ C_{36}^* &= \frac{D_I (C_{36}^{(2)} C_{33}^{(1)} \phi_2 + C_{36}^{(1)} C_{33}^{(2)} \phi_1)}{(C_{33}^{(2)} \phi_1 + C_{33}^{(1)} \phi_2) D_I + C_{33}^{(2)} C_{33}^{(1)}}, & C_{44}^* &= \frac{D_{II} C_{44}^{(2)} C_{44}^{(1)}}{(C_{44}^{(2)} \phi_1 + C_{44}^{(1)} \phi_2) D_{II} + C_{44}^{(2)} C_{44}^{(1)}} \\ C_{55}^* &= \frac{D_{III} C_{55}^{(2)} C_{55}^{(1)}}{(C_{55}^{(2)} \phi_1 + C_{55}^{(1)} \phi_2) D_{III} + C_{55}^{(2)} C_{55}^{(1)}}, & C_{66}^* &= C_{66}^{(1)} \phi_1 + C_{66}^{(2)} \phi_2 = \langle C_{66} \rangle \\ C_{45}^* &= \frac{D_{III} D_{II} (C_{44}^{(2)} C_{45}^{(1)} C_{55}^{(2)} \phi_1 + C_{44}^{(1)} C_{45}^{(2)} C_{55}^{(1)} \phi_2)}{((C_{55}^{(2)} \phi_1 + C_{55}^{(1)} \phi_2) D_{III} + C_{55}^{(2)} C_{55}^{(1)}) ((C_{44}^{(2)} \phi_1 + C_{44}^{(1)} \phi_2) D_{II} + C_{44}^{(2)} C_{44}^{(1)})} \end{aligned} \tag{25}$$

where C_{ij}^E denote components of the corresponding C_{ij}^* , they are lengthy and not shown here to save space. It appears that all components of the tensor are affected by interfacial stiffness except C_{66}^* . It is also clear to notice that C_{45}^* is affected by both D_{II} and D_{III} , while all others are affected by only one interfacial stiffness D_I , or, D_{II} , or D_{III} . It can easily be verifiable that as the interfacial stiffness goes to large value, all the components of effective stiffness tensor converge to the result obtained by Yu (2012) for perfect interface.

4. Results and discussions

In this section, the exact solutions of layered composites with imperfect interfaces are compared with the prediction obtained using 3D FEA by employing periodic boundary conditions in ANSYS. For 3D FEA, the interface between the two layers are modeled using interface element, INTER204/INTER205, for isotropic and monoclinic (anisotropic) material properties, respectively. First, let two isotropic layers be used to represent a periodically layered composite and also let the two layers have the same volume. The elastic modulus and Poisson's ratio of layer 1 are assumed to be 86 GPa and 0.22, respectively. The elastic modulus and Poisson's ratio of layer 2 are also assumed to be 4.3 GPa and 0.34, respectively. Let the tangential and normal interfacial stiffness be related as $D_{II} = 8 D_I$ and $D_{II} = D_{III}$. For 3D FEA, the SG is meshed to have 6400 elements (ANSYS Solid95).

The prediction for the longitudinal elastic moduli, E_1 and E_2 , are observed to be not affected by the interfacial stiffness as described in Eq. (18). Similarly, all Poisson's ratios (ν_{12} , ν_{13} , ν_{23}) are found to be not affected by interfacial stiffness (see Eqs. (22) and (23)). Moreover, Eq. (19) show G_{12} is independent of interfacial stiffness. The predictions of 3D FEA, for E_1 , E_2 , G_{12} and all Poisson's ratios, are also consistent with the predictions of exact solution. However, Fig. 3 shows that the predictions of transverse elastic modulus E_3 is significantly affected by the interfacial stiffness D_I . As the interfacial stiffness increases, the prediction of imperfect interface converges to the predictions obtained using perfect interface assumption. It is also found that interfacial stiffness D_{II} and D_{III} do not affect the transverse elastic modulus E_3 . The predictions of exact solution and 3D FEA show excellent agreement.

Fig. 4 shows the prediction of elastic shear modulus G_{23} is significantly affected by the interfacial stiffness D_{III} . It is also observed that as interfacial stiffness increases, the prediction of shear modulus G_{23} converges to the prediction of perfect interface. In this case, it is also noted that the interfacial stiffness D_I and D_{II} do not affect the prediction of the transverse shear modulus G_{23} . Similarly, the prediction of shear modulus G_{13} is found to be affected by interfacial stiffness D_{III} , see Eq. (20). This prediction is similar to the one obtained for the shear modulus G_{23} . The main difference is that G_{13} is affected by D_{III} while G_{23} is by D_{II} . For both cases, the predictions of exact solutions and 3D FEA show excellent agreement.

For more general case, let the layers exhibit orthotropic or monoclinic properties, obtained by assigning different orientations for material properties listed in Table 1. First, let the properties of the

Table 1 List of material properties

| E_1 (GPa) | $E_2 = E_3$ (GPa) | G_{23} (GPa) | $G_{12} = G_{13}$ (GPa) | $\nu_{12} = \nu_{13}$ | ν_{23} |
|-------------|-------------------|----------------|----------------------------|-----------------------|------------|
| 255 | 15 | 7 | 15 | 0.20 | 0.07 |

layers be obtained using 0 and 90 rotations, [0/90] and also let D_I be equal to 0.1 GPa and, D_{II} and D_{III} be equal to 0.8 GPa. Table 2 shows the predictions of exact solution obtained using Eq. (25) and 3D FEA. It shows that exact solution and 3D FEA are in a perfect agreement.

Although all the components of effective tensor except C_{66}^* are affected by interfacial stiffness as shown in Eq. (25), the effective compliance of [0/90] are not observed to be affected in a similar way as shown in Eq. (26)

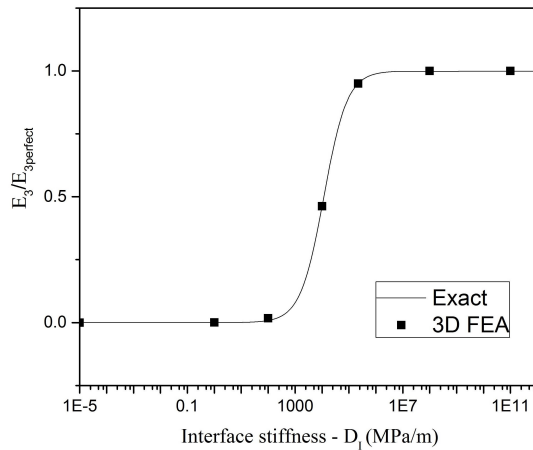


Fig. 3 Prediction of transverse elastic modulus E_3

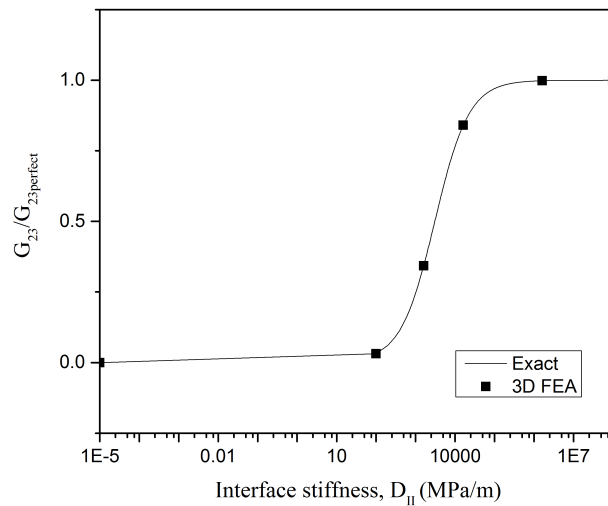


Fig. 4 Prediction of elastic shear modulus G_{23}

Table 2 Effective properties for [0/90] and [+/-45] layers

| Approach | $E_1 = E_2$ (GPa) | E_3 (GPa) | $G_{13} = G_{23}$ (GPa) | G_{12} (GPa) | ν_{12} | $\nu_{13} = \nu_{23}$ |
|-------------------|-------------------|-------------|-------------------------|----------------|------------|-----------------------|
| [0/90] Laminate | | | | | | |
| Exact | 120.46 | 0.09 | 0.73 | 15.00 | 0.025 | 0.140 |
| 3D FEA | 120.22 | 0.08 | 0.72 | 15.00 | 0.025 | 0.140 |
| 3D FEA/Exact* | 120.46 | 15.00 | 9.54 | 15.00 | 0.025 | 0.140 |
| [+/- 45] Laminate | | | | | | |
| Exact | 48.26 | 0.09 | 0.73 | 5.87 | 0.609 | 0.056 |
| 3D FEA | 48.14 | 0.08 | 0.72 | 5.85 | 0.605 | 0.052 |
| 3D FEA/"Exact**" | 48.26 | 15.00 | 9.45 | 5.87 | 0.609 | 0.052 |

Exact: Exact solution for perfect interface

$$\mathbf{S}^* = \begin{bmatrix} \frac{187}{22485} & -\frac{187}{899437} & \frac{757}{645750} & 0 & 0 & 0 \\ & \frac{187}{22485} & -\frac{757}{645750} & 0 & 0 & 0 \\ & & \frac{1201679}{18081000} + \frac{1}{D_I} & 0 & 0 & 0 \\ & SYMM & & \frac{11}{105} + \frac{1e9}{D_{II}} & 0 & 0 \\ & & & & \frac{11}{105} + \frac{1e9}{D_{III}} & 0 \\ & & & & & \frac{1}{15} \end{bmatrix} 10^{-9}. \quad (26)$$

The corresponding stiffness matrix can also be obtained by inverting the compliance matrix, where one can see C_{11}^* , C_{22}^* , C_{12}^* , C_{16}^* and C_{26}^* as function of interfacial stiffness, which is consistent with Eq. (25). Eq. (26) shows E_3 , G_{23} , and G_{13} varies with the interface stiffness D_I , D_{II} and D_{III} , respectively. Similarly, we can also obtain the prediction of [+/-45] laminate. Table 2 also shows the predictions of exact solution for [+/-45] are in a perfect agreement with the 3D FEA. The predictions of E_3 and G_{23} for various interfacial stiffness are similar to the one obtained for isotropic layers.

The current approach was also extended to four layers, for [0/90/0/90] and [45/-45/45/-45] laminates. The effect of imperfect interface on these laminates was also found to be similar to the the previous cases. Here it should be noted that interfacial stiffness between the layers was assumed to be the same. The predictions obtained for these cases are also the same as the one obtained for [0/90] and [+/-45], see Table 2.

5. Conclusions

The exact solutions of layered composites with imperfect interfaces are obtained using MSG based microemchanics approach. The interface between the layers is modeled using a linear traction-displacement model that assumes infinitesimal displacement jumps across the interface. The results of the prediction show that the interfacial stiffness does not affect longitudinal elastic moduli, all Poisson's ratios and shear modulus G_{12} . However, it significantly affects transverse Young's and shear

moduli. The predictions obtained using exact solutions show excellent agreement with the results of 3D FEA obtained by employing periodic boundary conditions. This study shows that it is worthwhile to consider the effect of imperfect interface for possible applications of layered composites particularly for structural design optimization, wave propagation and multiphysics properties of multifunctional materials. This study also indicates that it is more efficient to use the analytical approach than using the numerical approach which can be computationally demanding.

Acknowledgments

The authors acknowledge the support of Composite Design and Manufacturing HUB (<https://cdmhub.org/>) for successful completion of this assessment. The views and conclusions contained herein are those of the author and should not be interpreted as necessarily representing the official policies or endorsement, either expressed or implied, of the sponsors.

References

- Alvarez-Lima, R., Diaz-Diaz, A., Caron, J.F. and Chataigner, S. (2012a), "Enhanced layerwise model for laminates with imperfect interfaces part 1: Equations and theoretical validation", *Compos. Struct.*, **94**(4), 1694-1702.
- Alvarez-Lima, R., Diaz-Diaz, A., Caron, J.F. and Chataigner, S. (2012b), "Enhanced layerwise model for laminates with imperfect interfaces part 2: Experimental validation and failure prediction", *Compos. Struct.*, **94**(3), 1032-1037.
- Amor, M. and Ghozlen, M. (2007), "Frequency limit determination for the homogenization", *Mech. Res. Commun.*, **34**(5), 488-496.
- Backus, G. (1962), "Long-wave elastic anisotropy produced by horizontal layering", *J. Geophys. Res.*, **67**, 4427-4440.
- Bednarczyk, A. and Arnold, M. (2001), "Micromechanics based deformation and failure prediction for longitudinally reinforced titanium composites", *Compos. Sci. Technol.*, **61**(2), 705-729.
- Bendsoe, M. (1989), "Optimal shape design as a material distribution problem", *Struct. Optim.*, **1**(4), 193-202.
- Bensoussan, A., Lions, J. and Papanicolaou, G. (1978), *Asymptotic Analysis for Periodic Structures*, North-Holland, Amsterdam, the Netherlands.
- Berdichevsky, V. (2009), *Variational Principles of Continuum Mechanics*, Springer Berlin.
- Braga, A. and Herrmann, G. (1992), "Floquet waves in anisotropic periodically layered composites", *J. Acoust. Soc. Am.*, **91**(3), 1211-1227.
- Cecchi, A. and Sab, K. (2007), "A homogenized reissner-mindlin model for orthotropic periodic plates: Application to brickwork panels", *J. Sol. Struct.*, **44**(18), 6055-6079.
- Chen, Z., Yu, S., Meng, L. and Lin, Y. (2002), "Effective properties of layered magneto-electro-elastic composites", *Compos. Struct.*, **57**(1), 177-182.
- Ghosh, A. (1985), "Periodically layered composites for attenuation of dynamic loads", *Nucl. Eng. Des.*, **84**(1), 53-58.
- Hashin, Z. (1991a), "Thin interphase imperfect interface in elasticity with application to coated fiber composites", *J. Mech. Phys. Sol.*, **36**(6), 2509-2537.
- Jayatilake, I.N., Karunasena, W. and Lokuge, W. (2016), "Finite element based dynamic analysis of multilayer fibre composite sandwich plates with interlayer delaminations", *Adv. Aircraft Spacecraft Sci.*, **3**(1), 15-28.

- Jones, J. and Whittier, J. (1967), "Waves at a flexible bonded interface", *J. Appl. Mech.*, **28**, 103-128.
- Kamali, M. and Pourmoghaddam, S. (2016), "Three-dimensional analysis of multi-layer composite plates of arbitrary shape and boundary conditions with shear slip interfaces", *Mech. Adv. Mater. Struct.*, **23**(5), 481-493.
- Kim, B., Baltazar, A. and Kim, J. (2009), "Effective properties of multi-layered multi-functional composites", *Adv. Compos. Mater.*, **18**(2), 153-166.
- Kim, J. (2001), "Effective elastic constants of anisotropic multilayers", *Mech. Res. Commun.*, **28**(1), 97-101.
- Kim, J.S., Oh, J. and Cho, M. (2011), "Efficient analysis of laminated composite and sandwich plates with interfacial imperfections", *Compos. Part B: Eng.*, **42**(5), 1066-1075.
- Lan, M. and Wei, P. (2012), "Laminated piezoelectric phononic crystal with imperfect interfaces", *J. Appl. Phys.*, **111**(1), 013505.
- Le-Quang, H. and He, Q. (2008), "Variational principles and bounds for elastic inhomogeneous materials with coherent imperfect interfaces", *Mech. Mater.*, **40**(10), 865-884.
- Lebee, A. and Sab, K. (2010), "A cosserat multiparticle model for periodically layered materials", *Mech. Res. Commun.*, **37**(3), 293-297.
- Lim, T. (2009), "Out-of-plane modulus of semi-auxetic laminates", *Eur. J. Mech. A/Sol.*, **28**(4), 752-756.
- Manevitch, L., Andrianov, I. and Oshmyan, V. (2002), *Mechanics of Periodically Heterogeneous Structures*, Springer, Berlin, Germany.
- Massabo, R. and Campi, F. (2015), "Assessment and correction of theories for multilayered plates with imperfect interfaces.", *Meccan.*, **50**(4), 1045-1071.
- Milton, G. (2002), *The Theory of Composites*, Cambridge University Press, U.K.
- Munoz, V., Perrin, M., Pastor, M.L., Weleman, H., Cantarel, A. and Karama, M. (2015), "Determination of the elastic properties in CFRP composites: Comparison of different approaches based on tensile tests and ultrasonic characterization", *Adv. Aircraft Spacecraft Sci.*, **2**(3), 249-261.
- Norris, A. (1990), *The Effective Moduli of Layered Media: A New Look at an Old Problem*, Springer, New York, U.S.A.
- Santoyoa, E., Carrasqueroa, L., Rosadob, R., Sabinac, F., Ramosa, R. and Castilleroa, J. (2007), "Effective properties of periodic or non-periodic multilayered thermopiezoelectric composites", in "Rev. Cub. Fisica", **23**, 20-24.
- Wang, Q. and Yu, W. (2014), "A variational asymptotic approach for thermoelastic analysis of composite beams", *Adv. Aircraft Spacecraft Sci.*, **1**(1), 93-123.
- Wang, Y. (1999), "Nonlocal elastic analogy for wave propagation in periodically layered composites", *Mech. Res. Commun.*, **26**(6), 719-723.
- Yu, W. (2005), "A variational-asymptotic cell method for periodically heterogeneous materials", in "Proceedings of the ASME International Mechanical Engineering Congress and RD&D Expo", Orlando, Florida, U.S.A., November.
- Yu, W. (2012), "An exact solution for micromechanical analysis of periodically layered composites", *Mech. Res. Commun.*, **46**, 71-74.
- Yu, W. (2016), "A unified theory for constitutive modeling of composites", *J. Mech. Mater. Struct.*, **11**(4), 379-411.